

PAPER • OPEN ACCESS

## Modeling, Simulation and Experimental study on Giant Magnetostrictive Pump-Hydraulic System

To cite this article: Yapeng Zhao *et al* 2019 *IOP Conf. Ser.: Mater. Sci. Eng.* **592** 012065

View the [article online](#) for updates and enhancements.

You may also like

- [Vibration analysis and experiment of giant magnetostrictive force sensor](#)  
Zhiwen Zhu, Fang Liu, Xingqiao Zhu *et al.*
- [Characteristics of vibration energy harvesting using giant magnetostrictive cantilevers with resonant tuning](#)  
Kotaro Mori, Tadashi Horibe, Shigekazu Ishikawa *et al.*
- [Electromechanical coupling measurement of a new giant magnetostrictive structure for double-nut ball screw pre-tightening](#)  
Qingdong Wang and Mingxing Lin



**ECS**  
The  
Electrochemical  
Society  
Advancing solid state &  
electrochemical science & technology

**DISCOVER**  
how sustainability  
intersects with  
electrochemistry & solid  
state science research

# Modeling, Simulation and Experimental study on Giant Magnetostrictive Pump-Hydraulic System

Yapeng Zhao<sup>1</sup>, Xuyao Zhang<sup>1</sup>, Quanguo Lu<sup>2</sup>

<sup>1</sup>The 713th Research Institute of China Shipbuilding Industry Corporation, Zhengzhou, China

<sup>2</sup>Institute of Micro/Nano Actuation and Control, Nanchang Institute of Technology, Nanchang, China

Zypyapeng02@163.com

**Abstract.** In recent years, there have been growing attention for hydraulic actuators with smart materials. In this paper, a new type of giant magnetostrictive pump structure was designed and the experimental framework of giant magnetostrictive pump-hydraulic drive system was proposed. The dynamic model of giant magnetostrictive pump-hydraulic drive system was constructed. Thus, the output speed of output cylinder in this system under different preload was simulated and experimental study was carried out under the same conditions. The experimental results verified efficiency of the dynamic model to a large extent.

## 1. Introduction

Tefenol-D alloy which known as giant magnetostrictive material, its magnetostrictive coefficient can reach 1500 ~ 2000 ppm at normal temperature. This material is a kind of new functional material which offers large output force, high energy density, fast response speed and frequency bandwidth compared with piezoelectric ceramics in same length [1-3]. It widely used in many applications such as ultrasonic transducers, precision positioning, ultraprecision machining and fluid components [4-7]. Giant magnetostrictive pump (GMP) based on rare earth giant magnetostrictive material directly converts electrical energy into the reciprocating linear motion of the piston. Since the pump has the advantages of simple structure, easy miniaturization and precise control of output flow, Giant magnetostrictive pump becomes the focus of research [8][9].

Using hydraulic stroke amplification technology, Gerver developed a magnetostrictive laminated pump which input power is 25-30 W and the output power is 1 W [10]. Sirohi and Chopra have developed a compact hybrid hydraulic pump which can be driven by piezoelectric stacks, giant magnetostrictive rods or electrostrictive materials respectively. The pump had an output power of 2.5 W and a maximum output force of 138 N at a peak pumping frequency of 600-700 Hz [11]. CSA Engineering's Ryan C.S. developed a giant magnetostrictive hydraulic pump whose output power is more than 100 W. With a length of 102 mm, 25.4 mm diameter Terfenol-D driving, the best operating frequency of the pump is 200 Hz [12]. In this paper, a new type of giant magnetostrictive pump is developed, which has a large output flow and pressure. The hydraulic drive system which use giant magnetostrictive pump as power source is constructed. By dynamic modeling, simulation, and test analysis of hydraulic drive system, the dynamic characteristics of giant magnetostrictive pump-hydraulic drive system are studied.



## 2. Giant magnetostrictive pump-hydraulic drive system

As shown in Figure 1, Mechanical structure of the giant magnetostrictive pump has several major components: Terfenol-D rod, magnetizing coil, output shaft, spring, preload nut, piston assembly, reed valve assembly, pump body and head. When a certain current is loaded in magnetizing coil, the magnetic field will generate inside the coil. Terfenol-D rod generates magnetostriction under the effect of magnetic field and pushes the output shaft and piston assembly to produce displacement and force, finally achieves the conversion between electromagnetic energy and mechanical energy.

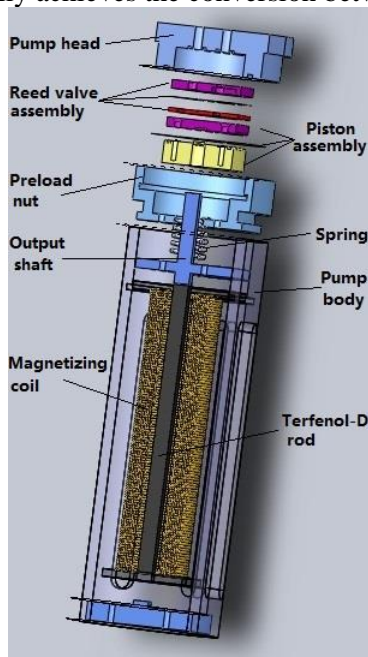


Figure 1. Exploded view of GMP

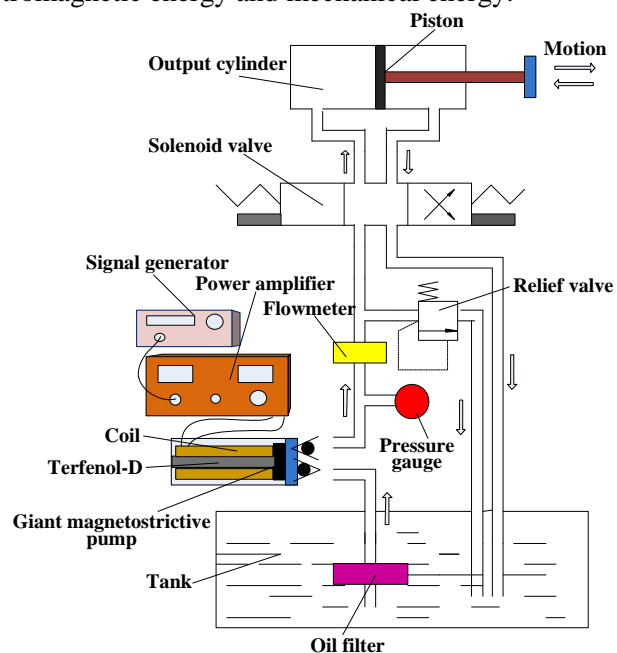


Figure 2. Frame diagram of GMP-hydraulic drive system

A spring is installed between output shaft and preload nut to form a preload mechanism. Adjusting upper and lower positions by rotating preload nut, the level of preload can be changed. The preload mechanism applies a certain preload on Terfenol-D rod, which makes Terfenol-D rod work in the linear range, as much as possible to increase magnetostrictive coefficient and improve electro-mechanical conversion efficiency. At the same time, preload mechanism provides a reliable return force for output shaft and piston assembly to achieve a linear reciprocating motion of piston assembly, finally resulting in a good pump action.

According to working characteristics of giant magnetostrictive pump, a small hydraulic drive system is established and the system frame is shown in Figure 2. In order to eliminate the impact of impurities and bubbles in oil, we set a grid-style oil filter in the tank. A pressure gauge and a flowmeter are installed in the outlet tube of giant magnetostrictive pump to test output pressure and output flow of the pump. A relief valve is set in the inlet tube of the output cylinder. When the output cylinder reaches the limit position and the relief valve is not open, the pressure of the system will rise abruptly. Then the relief valve will open automatically to prevent the system pressure increases. The return of output cylinder is controlled by a two-position four-way solenoid valve installed in the system.

In the test, SF-2 DDS type signal generator is used to generate sinusoidal signals of different frequency. These signals will be amplified by AE Techron 7224 power amplifier, then loaded on giant magnetostrictive pump.

## 3. Giant magnetostrictive pump-hydraulic drive system dynamic model

Since the giant magnetostrictive pump-hydraulic drive system is properly simplified, the schematic diagram of the system model is shown in Figure 3. The model can be analyzed from following aspects: pump chamber, check valve, tube and output cylinder and other aspects.

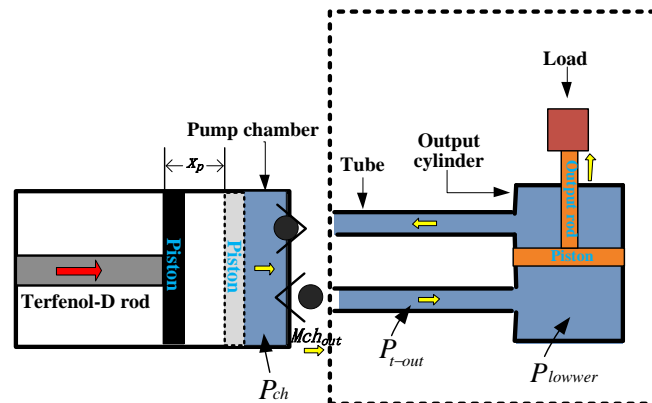


Figure 3. Schematic of GMP-hydraulic drive system

### 3.1. Flow field analysis of pump chamber

The pump chamber and output cylinder are connected by two tubes. The pressure of the two tubes is not identical at the same time, so we can distinguish the pressure of different positions in different tubes with different parameters.

Pump chamber working state

$$r = \begin{cases} 1 & r_{in} = 0, r_{out} = 1 \\ 0 & r_{in} = 0, r_{out} = 0 \\ -1 & r_{in} = 1, r_{out} = 0 \\ \text{null} & r_{in} = 1, r_{out} = 1 \end{cases} \quad (1)$$

Null is used to represent that the condition does not exist and it means that, in normal working condition, the two reeds of check valve do not open at the same time.

When  $r = 1$ , the pump is in discharge stage. The pressure changing function of pump chamber is

$$\dot{P}_{ch} = \beta \frac{A_{ch}\rho_{ch}\dot{x}_p - \rho_{ch}Q_{t1-out}}{\rho_{ch}A_{ch}(h_{ch} - x_p)} \quad (2)$$

Where,  $A_{ch}$  is cross section area of pump piston,  $x_p$  is displacement of pump piston,  $h_{ch}$  is height of pump chamber,  $\beta$  is liquid bulk modulus of elasticity.

When  $r = 0$ , the pump is in compression stage or expansion stage.

Then, the pump pressure changing function is

$$\dot{P}_{ch} = \beta \frac{\dot{x}_p}{h_{ch} - x_p} \quad (3)$$

When  $r = -1$ , the pump is in intake stage.

$$\dot{P}_{ch} = \beta \frac{A_{ch}\rho_{ch}\dot{x}_p + \rho_{ch}Q_{tN-in}}{\rho_{ch}A_{ch}(h_{ch} - x_p)} \quad (4)$$

Where  $\rho$  is liquid density in inlet tube,  $Q_{tN-in}$  is the input flow of pump or flow of inlet tube.

### 3.2. Flow field analysis of check valve

When  $r = 1$ , the pump is in discharge stage. It is easily get that

$$\dot{P}_{ch} = \frac{\beta}{\rho_{ch}A_{ch}(h_{ch} - x_p)} \left( A_{ch}\rho_{ch}\dot{x}_p - C \frac{8\pi\rho_{ch}(P_{ch} - P_{t1-out})r_v^3 l_v^3}{Eb_v h_v^3} \sqrt{\frac{2(P_{ch} - P_{t1-out})}{\rho_{ch}}} \right) \quad (5)$$

When  $r = -1$ , the pump is in intake stage. The pressure changing inside the pump is following as

$$\dot{P}_{ch} = \frac{\beta}{\rho_{ch}A_{ch}(h_{ch} - x_p)} \left( A_{ch}\rho_{ch}\dot{x}_p + C \frac{8\pi\rho_{ch}(P_{tN-in} - P_{ch})r_v^3 l_v^3}{Eb_v h_v^3} \sqrt{\frac{2(P_{tN-in} - P_{ch})}{\rho}} \right) \quad (6)$$

### 3.3. Flow field analysis of tube

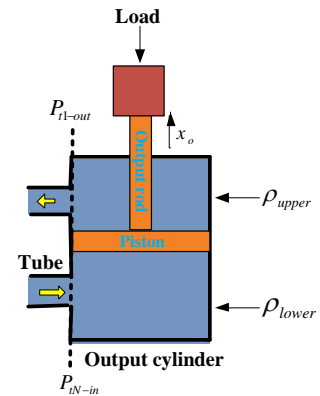
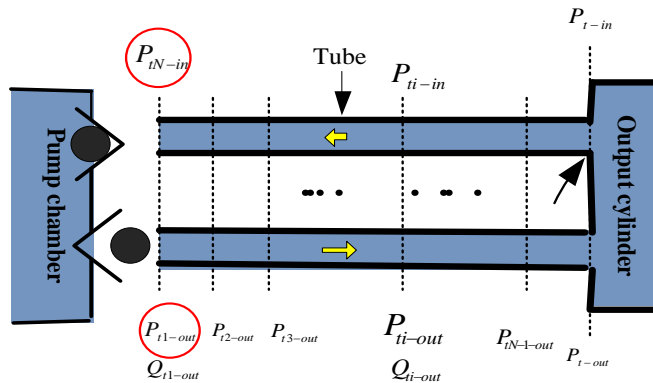


Figure 4. Lumped model of fluid flow through tube      Figure 5. Flow field model of output cylinder  
 As shown in Figure 4, the tube liquid pressure from pump chamber to output cylinder is noted as  $P_{t-out}$ , and the tube liquid pressure from output cylinder to pump chamber is noted as  $P_{t-in}$ . In order to study how the relationship between pressure and flow in the tube changes dynamically, we divide the tube into  $N$  parts.

According to momentum conservation law, the following equations is obtained

$$\dot{Q}_{ti-in} = \frac{NA_t(P_{ti-in}-P_{t(i+1)-in})-l_t A_t R_t \rho Q_{ti-in}}{l_t \rho} \quad i = 2,3, \dots, N - 1 \quad (7)$$

$$\dot{Q}_{ti-out} = \frac{P_{ti-out}-P_{t(i+1)-out}-\frac{l_t}{N} R_t \rho Q_{ti-out}}{\frac{l_t}{NA_t} \rho}, \quad i = 2,3 \dots, N - 1 \quad (8)$$

According to the momentum equation, we get the following equation

$$\dot{Q}_{tN-out} = \frac{(P_{tN-out}-P_{lower})A_t^2}{2\rho Q_{tN-out}} \quad (9)$$

$$\dot{Q}_{t1-in} = \frac{(P_{upper}-P_{t1-in})A_t^2}{2\rho Q_{t1-in}} \quad (10)$$

### 3.4. Flow field analysis of output cylinder

As shown in Figure 5, as same as the pressure in the end of the tube respectively, the pressure on the upper side of piston in output cylinder is denoted as  $P_{upper}$  and lower side of that is denoted as  $P_{lower}$ . The liquid density on the upper side of piston in output cylinder is denoted as  $\rho_{upper}$ , and on the lower side of that is denoted as  $\rho_{lower}$ . The length of output cylinder is denoted as  $l_o$ , the cross section area of output cylinder is denoted as  $A_o$ .

Assuming that initial position of the piston is in the middle of output cylinder, liquid mass above the piston changes like this

$$\frac{\rho_o A_o l_o}{2} = \rho_{upper} \left( \frac{l_o}{2} - x_o \right) A_o + M_{o-out} \quad (11)$$

Take the derivative of both sides, since  $\dot{M}_{o-out} = \rho_{upper} Q_{t1-in}$ , then

$$\dot{\rho}_{upper} = \frac{\rho_{upper} \dot{x}_o A_o - \rho_{upper} Q_{t1-in}}{\left( \frac{l_o}{2} - x_o \right) A_o} \quad (12)$$

Similarly, the density changing below the piston is

$$\dot{\rho}_{lower} = \frac{\rho Q_{tN-out} - \rho_{lower} \dot{x}_o A_o}{\left( \frac{l_o}{2} + x_o \right) A_o} \quad (13)$$

### 3.5. Dynamic model of piston in output cylinder

The dynamic equation of the piston in output cylinder is

$$(m_{op} + m_s) \ddot{x}_o + c_o \dot{x}_o + k_o x_o = (P_{lower} - P_{upper}) A_o - (m_{op} + m_s) g - F_{load} \quad (14)$$

Where  $m_{op}$  is mass of the piston in output cylinder,  $m_s$  is mass of the output rod in output cylinder,  $c_o$  is the damping coefficient of output cylinder,  $k_o$  is the stiffness coefficient of output cylinder,  $x_o$  is displacement of the piston,  $A_o$  is cross section area of the piston and  $F_{load}$  is the gravity of the load.

**4. Simulation and experimental analysis**

Under given parameters in giant magnetostrictive pump-hydraulic drive system, with the input current is 4 A and the preload is 5 MPa, 10 MPa and 15 MPa respectively, the output speed of output cylinder is simulated. The simulation results and experimental results are given as shown in Figure 6.

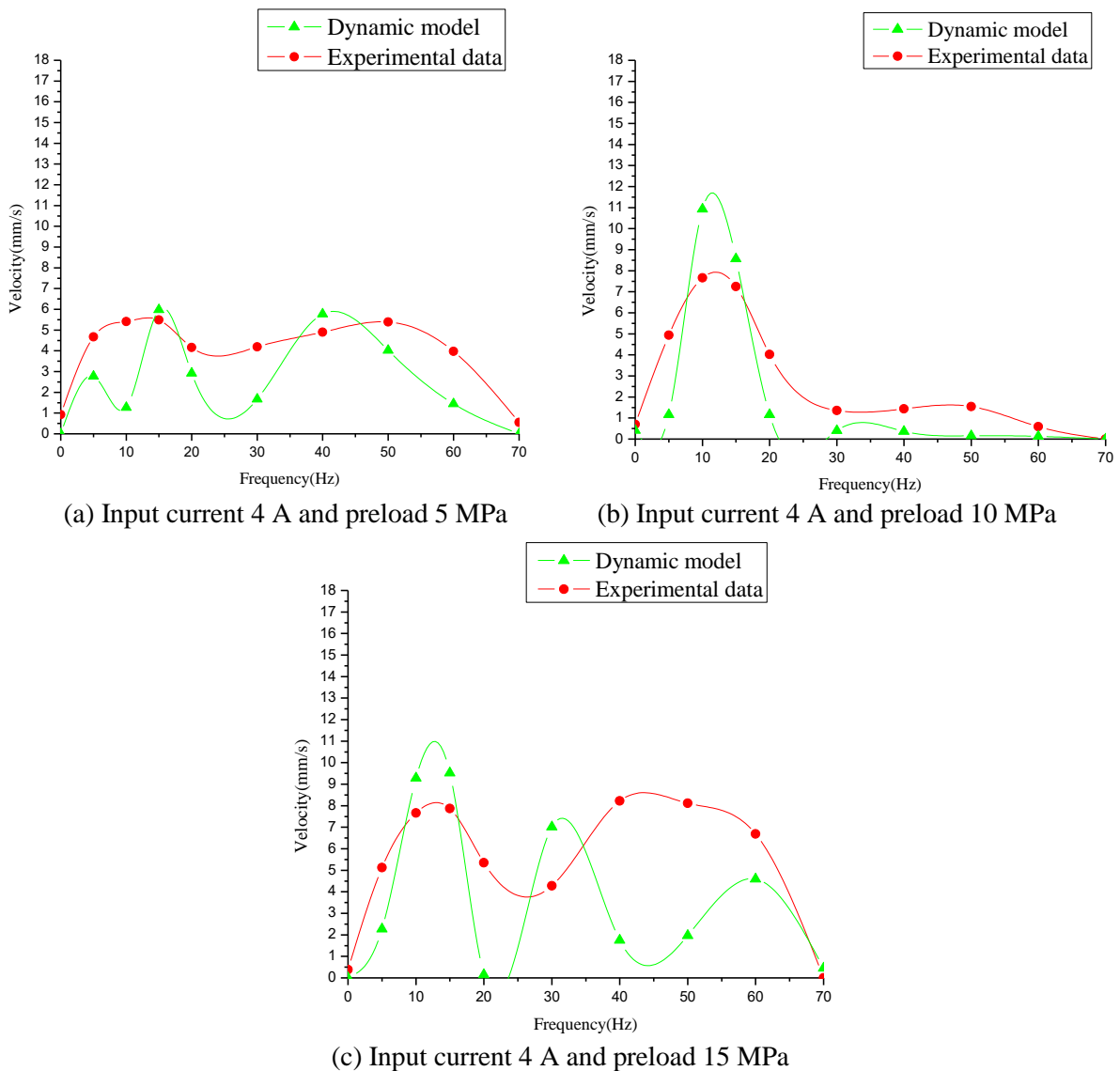


Figure 6. Comparison of experimental data and simulation results of dynamic model

The established dynamic model contains the effect of preload on output displacement of Terfenol-D rod, the inertia of liquid in pump chamber, the change tendency of liquid density in pump chamber, the change of pressure and flow rate in check valve and tube, the change tendency of liquid density in output cylinder, the inertia of piston movement and all of the above are related to the preload factor. Therefore, as shown in Figure 7, under the different preload, the change tendency of output speed in simulation results under the different frequency is very different.

When the preload is 5 MPa, the dynamic model simulation results show two peaks at 15Hz and 40Hz. The experimental results show that there are two peaks at 15Hz and 50Hz. The experimental

results are slightly delayed compared with the simulation results. However, the data is larger than the simulation results. When the preload is 10 MPa, the peak in simulation results and the peak in experimental data all appear at 10Hz, while the change tendency of both results under the different frequency is similar and their value are relatively close. When the preload is 15 MPa, the dynamic model simulation results show peak at 15Hz, 30Hz and 60Hz, while the experimental data appear at about 15Hz and 40Hz, and the numerical difference between corresponding data is large.

According to the dynamic model of giant magnetostrictive pump-hydraulic drive system, the dynamic behavior of output flow, check valve, tube and output cylinder are described. There are many factors that affect the dynamic model, including structural shape of tube and interface, the change of liquid density in output cylinder, the inertia of liquid in pump chamber, and the inertia of piston movement. Although there were some minor differences between the simulation results and experimental data, the experimental data verifies the established dynamic model to a large extent from the change tendency of output speed varies with frequency.

## 5. Conclusion

The giant magnetostrictive pump-hydraulic drive system involves a more complex multi-physics coupling. At first, the dynamic equations of pump chamber, check valve, tube and output cylinder in hydraulic drive system were modeling respectively. Using state space method, the dynamic model of giant magnetostrictive pump-hydraulic drive system is constructed by combing these equations. Comparing the numerical simulation results of dynamic model with experimental data, both results are close to each other when the input current is 4A and the preload is 10 MPa and the fitting degree between the curve of experimental results and that of simulation results is also good. The experimental data verifies the accuracy of the established dynamic model to a large extent.

## References

- [1] Li XC, Ding YT and Hu Y 2012 *Xiyou Jinshu Cailiao Yu Gongcheng/Rare Metal Materials and Engineering* 2045-2048
- [2] Lu QG, Zhao YP and Nie Q 2016 *Materials Science Forum* 943-951
- [3] John S, Sirohi J, Wang G and Wereley N M 2007 *Journal of Intelligent Material Systems and Structures* 1035-1048
- [4] Fang ZW, Zhang YW, Li X, Ding H and Chen LQ 2017 *Journal of Sound and Vibration* 35-49
- [5] Raghavendra A 2009 *Baltimore County: University of Maryland*
- [6] Wang M.D, Li D.S, Huang Y, Zhang C, Zhong K.M and Sun L.N 2013 *Fourth International Conference on Smart Materials and Nanotechnology in Engineering* 8793
- [7] Salzer S, Durdaut P, Robisch V, Meyners D, Quandt E, Hoft M and Knochel R 2017 *IEEE Sensors Journal* 1373-1383
- [8] Chaudhuri A and Wereley N 2012 *Journal of Intelligent Material Systems and Structures* 597-634
- [9] Ellison J A, Sirohi J and Chopra I 2004 *Proc. SPIE* 483-494
- [10] Gerber M. J 1998 *SPIE Conference on Smart Structures and Integrated Systems* 694-705
- [11] Ellison J, Sirohi J and Chopra I 2005 *Smart Structures and Integrated Systems* 274-289
- [12] Ryan C.S, Roland R.S and Michael F.C 2006 *2006 ASME International Mechanical Engineering Congress and Exposition* 435-443